Nationaal Lucht- en Ruimtevaartlaboratorium
National Aerospace Laboratory NLR

NLR-TP-99188

Review of aeronautical fatigue investigation in the Netherlands during the period March 1997 - March 1999

H.H. Ottens

Nationaal Lucht- en Ruimtevaartlaboratorium

National Aerospace Laboratory NLR

NLR-TP-99188

Review of aeronautical fatigue investigation in the Netherlands during the period March 1997 - March 1999

H.H. Ottens

This report is based on an article to be published in the proceedings of the 26th ICAF conference.

Division:	Structures and Materials
Issued:	April 1999
Classification of title:	Unclassified

Summary

A brief review is given of work performed in the Netherlands in the field of aeronautical fatigue. Where possible, applicable references have been presented.

Contents

(27 pages in total)

Review of aeronautical fatigue investigation in the Netherlands during the period March 1997 - March 1999

H.H. Ottens
National Aerospace Laboratory NLR
Anthony Fokkerweg 2
1006 BM Amsterdam
The Netherlands

1.1 INTRODUCTION

The present review gives a brief summary of the work performed in the Netherlands in the field of aeronautical fatigue, during the period from March 1997 until March 1999. The various contributions to this review come from the following sources:

- The National Aerospace Laboratory NLR
- The Faculty of Aerospace Engineering, Delft University of Technology (TU Delft)
- The Faculty of Mechanical Engineering, Eindhoven University (TU Eindhoven)
- Fokker Services
- Fokker Aerostructures
- Structural Laminates Industries (SLI)

The names of the principal investigator and their affiliation are presented between brackets at the end of each topic title.

1.2 LOADS

1.2.1 Determination of lateral gust loads (P.A. van Gelder, NLR)

Partly as a continuation of the “Fokker 100 Tail Loads Programme” that has been reported in previous ICAF meetings, NLR has carried out a research programme to test and validate newly in-house developed (unsteady) aerodynamic codes, especially with respect to the determination of lateral gust loads on aircraft. Calculations have been carried out with the Aero-elastic Simulation package (AESIM) for a Fokker 100 configuration and results will be compared with wind-tunnel data. The calculations were completed in 1998 and the final results will be reported in 1999.

1.2.2 Standard load sequences for aeronautical applications (P.A. van Gelder, NLR)

The National Aerospace Laboratory NLR has been actively involved, especially in the period between 1975 and 1992, with the creation and validation of standardised load sequences for fatigue analyses and testing.
In order to increase the accessibility, in terms of availability and application, and also to minimise the possibility of erroneous application of the data, all sequences (available at NLR) will be stored on one device (CD-ROM).
A database function will be added that will enable the generation of load/stress sequences for the appropriate stress levels from the basic data. Also an interface option for common crack-growth programs such as NASGRO (NASA) and CRAGRO (NLR) will supplied.
The relevant describing reports will be added as well to this CD-ROM in a digital format (PDF).
The CD-ROM is expected to be completed in 1999.

1.2.3 FAA flight loads programme (P.A. van Gelder, NLR)

For the ageing aircraft programme FAA has installed Flight Data Recorders in a number of transport aircraft for load and usage monitoring. NLR was asked to advice FAA on this programme. One of the NLR tasks is to investigate whether the sampling rates that are currently used by onboard Flight Data Recorders is sufficient to supply statistically realistic and relevant loads data (cg-accelerations) and usage data (e.g. flap deflections). NLR carries out this investigation using NASA supplied flight data sampled at a high rate (20-100 Hz). This project is carried out as a co-operation between NLR the FAA and the Netherlands Airworthiness Authorities RLD.

1.2.4 Fatigue loads/usage monitoring of military aircraft

a. Structural fatigue load monitoring of RNLAF F-16 aircraft (D.J. Spiekhout, NLR)

The fatigue load monitoring programme of F-16 aircraft of the Royal Netherlands Air Force (RNLAF) has been continued. In the previous programme three aircraft per squadron were equipped with a four channel digital solid state recorder measuring wing root bending moment and three additional load quantities This programme is gradually phased out and replaced by the FACE system
The “Fatigue analysing and Air Combat Evaluation system (FACE)” was developed by RADA Electronics Industries Ltd. In Israel and will be installed in all RNLAF F-16 aircraft. To date in about 60% of the RNLAF fleet a FACE system has been installed. The FACE system allows a more extensive load monitoring on individual aircraft bases. Quantities measured to monitor structural fatigue loading include strains in five different structural locations: two indicative for wing root bending and outer wing bending, two at the rear fuselage dealing with horizontal and vertical tail loads and one in the fuselage center section indicative for fuselage bending. With these strain gages a number of flight parameters are measured simultaneously. The FACE system is also used to monitor engine loads and usage.
Apart from the continuous load and usage monitoring programme the FACE system is capable to do campaign measurements. The FACE system and its possibilities are described in Ref. 1.

b. Maritime Patrol Aircraft, P-3 Orion (A.A. ten Have, NLR)

NLR has developed software to perform fatigue life calculations of the P-3 Orion maritime patrol aircraft These calculations provide the operator with a validated fatigue life indicator for the most critical wing location of the P-3 Orion airframe structure. This package is currently in use by the RNLN (as “PLEBOI”), the Spanish Airforce (as “SAFORI”) and the Portuguese Airforce (as “POLICAL”). NLR performs structural data recording activities in RNLN and PoAF P-3 Orion to support theoretical fatigue life calculations

c. Transport Aircraft, C-130 Hercules (R.P.G. Veul, NLR)

The Royal Netherlands Airforce operates two C-130H-30 Hercules aircraft that were delivered in 1994/1995. In order to optimize operational and maintenance aspects, NLR is setting up tailored C-130 structural life monitoring procedures. An in-flight data acquisition system will be installed in each of the C-130 Hercules airframes, generating operational usage and service loads data.

1.2.5 Helicopters (A.A. ten Have, NLR)

a. Lynx helicopter (A.A. ten Have, NLR)

To achieve Lynx life extension and to monitor and control maintenance of the main rotor and sponson (the Lynx undercarriage support structure) loads, the Royal Netherlands Navy RNLN has decided for a fleetwide installation of a multi-channel structural data recorder system, called the AIDA system. This AIDA system will also cover and replace engine cycle counter functionalities. NLR has provided extensive support to the RNLN by defining the AIDA functional specification, generating user-requirements and source selection input data, co-developing desired AIDA functionalities, performing airworthiness tests, and developing Host Station Software.

Current status as of April 1999, is that production AIDA systems are being delivered, Lynx airframes are being modified, and the AIDA certification process is being finalized. Developing the Host Station Software is still underway.
Apart from the RNLN, German and Brazilian military operators also consider installation of this NLR developed AIDA system for their Lynx fleets. To support these operators in their decision-making process, NLR has provided input.

b. Bo-105, Chinook, Cougar helicopter (A.A. ten Have, NLR)

NLR has supported the Royal Netherlands Airforce RNLAF with structural integrity issues concerning the Bo-105, Chinook and Cougar. With respect to the Bo-105, these activities concern service life extension aspects of ageing airframes, with respect to the other helicopter types they concern optimization of new helicopters structural integrity issues. In particular, corrosion and crack logging and administrative usage monitoring procedures are under study.

1.3 ENGINES

1.3.1 Engine usage monitoring

a. Pratt & Whitney F100 engine (J.H. Heida, J.F. Slauerhoff, NLR)

Since 1991, NLR performs operational engine usage monitoring of the Pratt & Whitney F100 engines installed in F-16 aircraft. For this purpose, a number of multi-channel data-acquisition systems have been installed in the RNLAF F-16 fleet registering parameters such as pressure altitude, calibrated airspeed, engine rotational speed and power lever angle. Engine damage accumulation is then calculated from the recorded engine cycles using specific algorithms. Furthermore, flight time and hot time envelopes (time spent in certain Mach number versus altitude regions) are determined to gain more insight in the RNLAF F100 mission profile. To date, more than 11000 RNLAF F-16 sorties have been collected. On a routine basis, this operational RNLAF engine data is transferred to the engine manufacturer for evaluation purposes and could be used as a basis for tailored engine maintenance procedures, e.g. affecting inspection intervals or retirement lives.
From 1997, the Fatigue Analysing and Air Combat Evaluation system (FACE) is being introduced in RNLAF F-16 aircraft. FACE is a comprehensive maintenance management and flight debriefing system developed by RADA Electronic Industries Ltd in Israel. This system enables the recording of approximately 100 engine parameters of which a representative selection will be made in 1999. Ad-hoc campaign measurements will always allow other parameters to be temporarily monitored.

b. Rolls Royce Gem 42 engine (A.A. ten Have, NLR)

On a routine basis and employing four NLR developed engine cycle counters, NLR supports the Royal Netherlands Navy RNLN with Cyclic Life Control of their Lynx Gem engines. Currently, the RNLN is the only Lynx operator benefiting from tailored exchange rate in Gem engine maintenance procedures. In the near future the engine cycle counting is included in the AIDA system and the separate cycle counters will be phased out.

1.3.2 Life assessment of engine components (T. Tinga, NLR)

In order to do an accurate life assessment of a gasturbine component it is necessary to have detailed information on the gas turbine loads, thermal, aerodynamic and mechanical loads, and on the resulting stresses in the component.

The total loading of gas turbine components has two major contributions: thermal loading and mechanical loading. The loading of stationary (non-rotating) components like vanes is mainly thermal, caused by variations in temperature of the hot gas stream in which the components operate. Rotating components have additional mechanical loading, where the centrifugal loading due to the high rotational speed of the components is the most important contribution. At the NLR a method has been developed to determine both the thermal and centrifugal loading of any gas turbine component for any mission.

The basis of the analysis method is the Gas Turbine Simulation program (GSP), developed at the NLR. GSP performs a transient (gas path) analysis of a mission using power settings and flight conditions as input and giving, among others, gas temperatures, pressures and mass flows as output (see figure 1). The gas stream results of the GSP calculation are then used in a finite element (FE) analysis to calculate the temperature distribution in the component. The results of this thermal analysis are combined with the rotational speeds calculated by GSP to determine the stresses and strains in the component. Finally, the obtained stress spectrum is used to perform a life assessment of the component, which completes the analysis. The method has been applied to a real component, in this case a 3rd stage turbine blade of an F100-PW-200 turbofan engine.

1.3.3 Detailed analysis of engine components

a. Aerothermal loads analysis on engine components (R. Hagmeijer, NLR)

The theoretical aerodynamics department of NLR is responsible for providing thermal and aerodynamic loads on components due to the aerothermodynamics of the hot gas flow. The analysis is divided into two parts:

1) Computational Fluid Dynamics (CFD).
Based on solution of the 3D Reynolds-averaged Navier-Stokes equations, the thermal and mechanical loads are determined along the component boundaries. The set of five partial differential equations describes conservation of mass, momentum and energy respectively, for viscous compressible fluids. Accurate solution of a discretisation of this equation set is carried out by employing sufficiently dense grids to resolve all the relevant flow phenomena. Particularly, the heat transfer from the flow to the engine components is completely determined by the detailed shape of the temperature profile inside the boundary-layer. Extensive knowledge about the required grid resolution is available and employed. Until present CFD is carried out using commercially available codes on workstations. It is foreseen that one of these codes will be implemented on the NEC SX-5 supercomputer at NLR during 1999.

2) Asymptotic analysis.
To support design, verification and validation of other tools employed, e.g. CFD and physical experiments, an asymptotic analysis is carried out. Such analysis is based on asymptotic analysis of the 3D Navier-Stokes equations in boundary-layers where the flow field may locally satisfy similarity conditions. For example, the heat transfer from the flow to a stagnation point in the engine is predicted accurately by means of such asymptotic theory.

b. Thermal and thermo-mechanical analysis of engine components (A. de Boer, NLR)

In the framework of several projects on gasturbine components transient as well as steady state thermal analyses are carried out at NLR. The heat transmission coefficients that determine the heat flux from the gas flow to the gasturbine component are obtained from (in house) CFD analysis. The analysis may include internal component cooling.
Temperature dependent material properties such as the heat conduction coefficient and the specific heat are taken into account. At NLR thermal analyses are carried out with the finite difference program ESATAN and the finite element programs CFX, MARC and B2000. CFX allows a coupled CFD-thermal analysis. MARC is a commercial available structural finite element program. B2000 is a highly modular finite element program, which is used by NLR as a testbed for new developments and evaluation of (new) theories. PATRAN is used as geometry modeller and mesh generator for the structural finite element models. The heat transmission coefficients and corresponding surface co-ordinates obtained from CFD analyses can be read in PATRAN and interpolated to the structural node co-ordinates automatically. At NLR a mechanical-electrical 3D measuring device is available to measure geometries of gasturbine components with an accuracy of $1.5.10^{-5}$ m.

Thermo-mechanical analyses using the aerothermal loads and the thermal analysis results as input. For the thermo-mechanical stress analyses it is not required to use the same mesh as for the thermal analyses. Within PATRAN there are features to map the thermal distribution field from the thermal finite element mesh on the finite element model for the stress analyses.
At NLR thermo-mechanical analyses are carried out with MARC or with B2000 for new developments. In the case of transient thermal analyses stress distributions are calculated for certain (interesting) time steps. In these analyses temperature dependency of the material properties (Youngs' modulus, expansion coefficient) can be taken into account. Creep is taken into account when appropriate. To this end a time and temperature dependent creep function must be defined in a MARC user subroutine. The parameters for this function can be measured in the NLR material laboratory.

The calculation of the heat transmission with CFD as was described, was validated with experiments carried out at the Von Karman Institute and published in Ref. 2. It concerns the heat transfer to a turbine blade, a 2D turbine cascade (see figure 2). The calculated and measured heat transfer (represented by the Stanton number) for different Reynolds numbers are presented in figure 3. It can be concluded that in the region where the flow is clearly laminar, the difference between the computed and experimental heat transfer is small for the two larger Reynolds numbers, but increases to about 20% for the smallest Reynolds number.

The procedure for thermal and thermo-mechanical analyses of a turbine blade with cooling channels and the with ENFLOW computed heat transfer as input is evaluated for the VKI blade. To this end the 2D geometry has been extended to a prismatic 3D model with 5 cooling channels. A typical steady state temperature distribution is depicted in figure 4. Due to the presence of cooling channels there exists a temperature gradient in the blade cross section at steady state. The resulting thermal stresses in the blade are presented in figure 5. Effects of centrifugal loads and creep behaviour on the stress and strain distribution are studied, too.

1.3.4 Behaviour of thermal barrier coatings under a thermal loading (M.F.J. Koolloos, TU Eindhoven, NLR)

The failure mechanism of thermal barrier coatings (TBCs) subjected to a thermal load is still not entirely understood. Thermal stresses and/or oxidation cause the coating to fail and hence must be minimized. During the present investigation TBCs with a thickness of 0.3, 0.68 and 1.0 mm were sprayed which withstood the high thermal stresses during thermal cycling. Owing to the substantial thickness the temperature at the top coat / bond coat interface was relatively low, resulting in a low oxidation rate. Furthermore, bond coats were pre-oxidized before applying a top coat. The performance of the TBCs during three different thermal loads was investigated. These loads were: thermal shock (short cycles, top coat surface is heated by flame), thermal cycling (long cycles, top coat surface is heated by flame), and furnace testing (long cycles, entire specimen is heated) The thick TBCs applied during this research exhibited excellent thermal shock resistance but performed very poor during furnace testing. A pre-oxidation treatment of the bond coat increased the lifetime during thermal loading where oxidation was the main cause of failure. Results are presented in figures 6 and 7 and in Ref. 3.

1.3.5 Modelling of thermal barrier coatings (M.F.J. Koolloos, TU Eindhoven, NLR)

Finite Element (FE) models that take into account the bond coat pre-oxidation and interface roughness were used to calculate the stresses occurring during thermal shock and furnace testing. The global-local approach was used. First the temperature and stress profile on a macroscopic scale were calculated. Next a small piece was excerpted from the global model. A new fine mesh was generated including a rough interface with very fine elements allocated for an oxide layer. The FEM analysis of the thermal shock process gives a first impression of the stress conditions on the interface undulations during thermal loading, but further development is required. The FEM analysis of the furnace testing elucidated that delamination occurred owing to stress concentrations at the free edge of the specimen.
The experimental program is entirely performed at Eindhoven University of Technology, Department of Mechanical Engineering, Section Thermal Spraying (J.M. Houben)

1.4 FATIGUE AND DAMAGE TOLERANCE STUDIES

1.4.1 Fatigue of riveted lap joints (J.J.M. de Rijck, J. Homan, S.A. Fawaz, J. Schijve, A. Vlot, TU Delft)

Investigation on riveted lap joints as reported in the previous review were continued. The following topics have been studied.

a. Effect of the squeeze force on fatigue life

Experiments were carried out on GLARE specimens. The squeeze force has similar effect as previously shown for 2024-T3 lap joints, i.e. increasing of the squeeze force has a significantly favourable effect on the fatigue life. The fatigue lives for GLARE specimens, however, are much longer than for 2024-T3 specimens.

b. Correlation between the rivet squeeze force and the driven rivet head dimensions.

Manufacturing riveting machinery in the industry is equipped for displacement controlled riveting. The aim of the present investigation is to correlate the driven head dimensions (height and diameter) to the rivet squeeze force in order to check the rivet force as it was applied in production, and in this way to check the fatigue quality of riveted joints. Specimens have been made with the rivet diameter, rivet length, type of rivet and rivet materials as the variables. For each combination a range of squeeze forces was used. The correlation between squeeze force and driven rivet head dimensions is promising. Co-operation with Airbus industries should be mentioned.

c. Fatigue crack growth in riveted lap joint

The investigation reported in the previous Review has been continued. Previous work has been reported in the doctor thesis of Fawaz (Ref. 4) see also (Ref. 5). The present work is concentrating on stress intensity factors of fatigue cracks with oblique crack fronts and crack interactions of such cracks in adjacent holes in sheets under combined tension and bending. Experimental data were obtained on crack growth rates, crack shape development and crack interaction effects for fatigue cracks starting from different initial shapes in 2024-T3 sheet specimens with an array of holes. Although the fracture surfaces were quite tortuous, the crack growth history could be reconstructed by using marker loads introduced by reducing the maximum stress of the constant-amplitude baseline cycles. Crack growth histories were reconstructed for cracks smaller than 1 mm (sheet thickness 2 mm). In the analytical part K-values were calculated for part-elliptical through cracks emanating from an array of holes subjected to remote tension and bending, and pin loading. The 3-dimensional virtual crack closure technique (3D VCCT) is used. Calculations for different crack shapes were made. Interactions between cracks of adjacent holes were studied by comparison to K-values for cracks from single holes. The comparison indicated that such interactions will become significant only late in the fatigue life. Application of the new K-values to prediction of the fatigue life showed a 10% underestimation of the life.

1.4.2 Fractography to study interaction effects during variable-amplitude loading (J. Schijve, TU Delft)

Fatigue crack growth tests were carried out on 2024-T3 and 7075-T6 central cracked specimens, described in Ref. 6. Variable-amplitude (VA) load spectra were used with periodic overload (OL) cycles added to constant-amplitude (CA) cycles. The fatigue fracture surfaces were examined in the SEM to obtain more detailed information on crack growth contributions of different load cycles. The striation patterns could be related to the load histories. An example is shown in the figure 8. SEM observations were associated with delayed retardation, the effect of 10 or a single OL on retardation, crack growth during the OL cycles, and crack growth arrest after a high peak load. Fractographs exhibited local scatter of crack growth rates and sometimes a rather tortuous 3d geometry of the crack front. Indications of structural sensitive crack growth under VA loading were obtained. Fractography appears to be indispensable for the evaluation of fatigue crack growth prediction models in view of similarities and dissimilarities between crack growth and VA and CA loading.

1.4.3 Comparison of the damage tolerance behaviour of two aluminium alloys (G. Jay, J. Schijve, TU Delft)

Various properties of 2024-T3 and 2024-T3A are compared. The second alloy was developed by Pechiney as a replacement of the first one. The test program includes static and fatigue tests (constant-amplitude and flight-simulation). Specimens to be used include blunt notch specimens, center cracked specimens and riveted joints (study of multiple-site damage). The first constant-amplitude fatigue crack growth results indicate that 2024-T3A is superior to 2024-T3.

1.5 FULL SCALE FATIGUE TESTS

1.5.1 Fokker 50 and 100 fatigue and damage tolerance tests (J.J. Veenstra, Fokker Services)

After completion of the fatigue and damage tolerance tests at 180,000 flight cycles, the residual strength tests and the tear down inspection programme, the structural inspection programmes of the Fokker 70/100 and Fokker 50/60 are now in the process of being completed by Fokker Services.

With the Fokker 50 and 100 fatigue test results also a verification programme is started on the fatigue inspection programmes of the F27 and F28 aircraft versions. Moreover these fatigue test results will be considered in the Ageing Aircraft programmes on Repair Assessment and on Widespread Fatigue Damage.

Continuous support and development of Non-Destructive Inspections techniques for fatigue and damage tolerance inspection tasks is provided for by ASNT level III specialists.

1.5.2 Fokker 60 fatigue and damage tolerance tests (N.J. Fraterman, Fokker Aerostructures)

The Fokker 60 is a derivative of the Fokker 50 propjet; the major changes consists of a stretched fuselage, higher design weights, increased cruise speed and a large cargo door (3*2 meter) in the forward fuselage. Due to these structural modifications the fatigue spectra has changed to such an extend that additional fatigue and damage tolerance tests were required for the certification of the Fokker 60 according to JAR 25. The airworthiness authorities required additional fatigue tests for areas, which were subjected to considerable higher fatigue loads than the Fokker 50, areas with newly designed structures and/or areas where the original Fokker 50 tests could not be extrapolated any further. The resulting test programme consisted of the wing-fuselage lugs, a stringer run-out in the lower wing skin and a section of the large cargo door plus surround have been tested successfully and have been reported in the ICAF review of 1997.

One of the component tests represents a fatigue critical panel joint in the lower skin of the outer wing. The fatigue spectrum consists of flight loads due to gust/ manoeuvre and ground loads due to taxi/ landing. This area is designed and certified as a multiload-path structure and will therefore be tested for two and a half life times (=235000 FC) of which the last half life will be run with artificial cracks in order to verify the damage tolerance behaviour. He testpanel showed a crack in the cooling plate after approximately 40000 FC, which was repaired after monitoring the crack growth. The repaired panel has been tested for 92000 FC and a small crack has been found on another location. The slow propagation of this crack will be monitored, while the test on the panel is continued till a total of 235000 FC.

Another component test represents the mainframe, which is part of the wing-fuselage connection (see figure 9). The fatigue spectrum consists of flight loads due to gust/ manoeuvre plus cabin pressure and ground loads due to taxi, turning, landing impact and braking. The upper part of the mainframe has been designed and certified as a slow crack growth structure. Therefore it will be tested for two lifetimes (=180000 FC); thereafter artificial cracks of 0.05” will be inflicted at critical locations and the test will be continued for one and preferably for two lifetimes in order to demonstrate the slow crack growth behaviour. After 180000 FC a crack was discovered in a section of the machined mainframe. Investigations of the fracture showed that the crack was caused by an illegal hole that was drilled by accident and was surprisingly not discovered during the quality inspections. Microscopic analysis of the crack surface revealed that the crack has been initiated at ~90000 FC and propagated slowly until it was found at 180000 FC. The fact that the mainframe with the illegal hole sustained 180000 FC confirmed that the design was capable of handling extreme production defects. The cracked mainframe was replaced by a mainframe with artificial cracks of 0.05" at a number of critical locations in order to verify the damage tolerance behaviour. Up to April 1999 the mainframe with artificial cracks has been subjected to 60000 FC and none of the cracks did show any propagation. The mainframe will be tested till 180000 FC.

1.5.3 Thermoplast Main Undercarriage doors in the Fokker 50 (N.J. Fraterman, Fokker Aerostructures)

In order to gain experience in designing and building structural components in thermoplast CRFP-PPS the existing Aluminium Main Undercarriage (MUC) doors of the Fokker 50 were re-designed into CFRP-PPS version by Fokker Aircraft and Fokker Aerostructures. According to this design Fokker Special Products, using special developed forming and welding technology built one demonstrator. In order to be able to execute a service trial, a certification programme was agreed with the Dutch Airworthiness Authorities, which was based on a combination of tests and analysis. The test programme contained a full-scale static test on the door, static tests on samples and fatigue tests on a number of joints, including the welded joints. The fatigue tests on the welded joint showed a good behaviour in shear, but showed limited capability in tension. The fatigue properties were sufficient for the Fokker 50 MUC door design, but could be a limitation for other designs.

1.5.4 Testing the center section of a composite stabilizer (H.G.S.J. Thuis, NLR)

As part of a composite stabilizer technology programme a number of static and fatigue tests have been carried out on a "4-meterbox": a structurally complete composite center section of a stabilizer for the Fokker 100 aircraft (see figure 10). The purpose of the test program is to verify:

a. the dynamic behaviour as determined by analysis
b. the strain distribution as determined by analysis
c. the "no damage growth concept" during fatigue loading
d. ultimate load capability with Barely Visible Impact Damage (BVID)
e. the damage tolerance behaviour

During the tests the "4-meterbox" was attached to a full size vertical stabilizer. The vertical stabilizer was connected to a rigid test frame. A number of hydraulic actuators (ten for the static tests and twelve for the fatigue tests) were used to introduce the appropriate loads. The overall test program contained a number of static tests at elevated temperature (80 ˚C) and increased humidity (85 % R.H). During these tests the "4-meterbox" was placed in an environmental chamber (7 x 3 x 2.5 m).

Two preliminary tests were carried out at ambient conditions and were reported in the previous ICAF review

Test no 1: Dynamic test

Test no 2: Static strain survey to Limit Load

After these tests the "4-meterbox" was saturated in the environmental chamber. During saturation the conditions in the chamber were 80 ˚C and 85 % RH. It required 10 months to reach a sufficient level of saturation.

Test no 3: Fatigue test

The fatigue test was performed at room temperature. An equivalent of 90000 flights (1 lifetime) was tested using a load enhancement factor of 1.18. The fatigue load sequence was reduced by omitting all small cycles, leading to an average of 2.5 cycles per flight. The fatigue test was completed successfully, no significant damage occurred.

After the fatigue test the "4-meterbox" was saturated again and two static tests were performed in the hot-wet condition
Test no 4: Static test to Ultimate Load with BVID's
Test no 5: Static test to Limit Load with Visible Damages
Both tests were carried out without significant increase of the damages.

In the original test program static tests on the specimen with significant damages (failure of the front spar) were foreseen. It was decided, however, to keep the specimen intact to be able to use the specimen for tests in the future.

1.6 AGEING AIRCRAFT

1.6.1 Structural Maintenance of Ageing Aircraft (SMAAC) (W.J. van der Hoeven, NLR)

The NLR participates in the Brite Euram programme "Structural Maintenance of Ageing Aircraft (SMAAC)". The programme started in 1996 and is sponsored by the Commission of the European Union. The activities of NLR were reported in the previous ICAF review. The work done in the last two years is:

a. Fractography of pressure cabin MSD (R.J.H. Wanhill, NLR)

Multiple Site Damage, MSD, fatigue initiation and early crack growth were fratographically investigated for fuselage longitudinal lap splices from three aircraft types, of which two from service (Fokker F 28, BAC 1-11) and one from a full-scale test (Fokker 100). The results were compared with those from a NASA investigation of a Boeing 747-400 full-scale test. The most MSD-critical rivet row was the upper one in the outer sheets of the lap splices. However, other rows were susceptible, especially the lower one in the inner sheets.
Fatigue initiation lives appeared to vary widely. However, there was no evidence from the series aircraft that corrosion was involved in crack initiation. Early crack growth rates were above 10^{-8} m/ cycle, which is significant for two reasons: (a) one should not expect differences between 'short' and 'long' crack behaviour, and (b) it makes questionable the usefulness of testing sub-scale specimens, which show much lower early crack growth rates.
More details are provided in the paper in the ICAF 1999 Conference Proceedings.

b. Effect of precorrosion on the fatigue life of riveted lap joint specimens (L. Schra, W. van der Hoeven, NLR)

The effect of precorrosion on the fatigue life of riveted lap joint specimens was studied. Riveted lap joints were made of 1.2 mm thick Alcad 2024 T3 sheets. The joints were representative for the longitudinal joint in medium sized jet aircraft. After drilling the rivet holes, but before riveting the sheets were precorroded. The precorrosion conditions were those described in ASTM G85, Annex 2, see for example figure 11 and resulted in some corrosion of the cladding layer close to the rivets and a moderate pitting attack inside the rivet holes.
After precorrosion, the specimens were riveted and fatigue tested to failure. During the fatigue test the specimens were loaded under constant amplitude loading since this type of loading simulates the cyclic stress variation in the fuselage skin due to cabin pressurisation. The fatigue lives were determined for three maximum stress levels: 80, 100 and 120 MPa. In addition, tests were done on uncorroded specimens. From the results, it was concluded that fatigue cracks initiate at the corrosion pits, but that the corrosion damage had no effect on the fatigue life of the joints (see figure 12).

c. Full-scale fuselage panel tests (R.W.A. Vercammen, NLR)

During the SMAAC project, residual strength tests were performed on three curved fuselage panels with artificial damage. The panels were supplied by the SMAAC partners Deutsche Aerospace and Alenia. The tests were carried out in the fuselage panel test rig of the NLR. In this test rig, the loads due to cabin pressurisation can be simulated. The hoop loads are introduced by pressurisation of the pressure chamber

and the axial loads are introduced with an actuator. In the panels, saw cuts were made to simulate the presence of Multiple Site Damage. The damage consisted of a lead crack and many small cracks at the rivet holes in front of the lead crack. Before the static tests, the panels were loaded in fatigue to sharpen the tips of the lead crack.
During the residual strength test, only loads due to cabin pressure was increased until failure. The tests were successful in the sense that all panels sustained their ultimate design loads.

d. Crack initiation and crack growth models for MSD (F.P. Grooteman, NLR)

An MSD model for determination of the inspection intervals, threshold and follow-on inspections, for lap joints has been developed. It consists of a crack initiation and a crack growth model, both dealing with the MSD situation in which neighbouring cracks have influence on the crack initiation and growth.

The crack initiation model is based on P-S-N curves concept, where the S-N curves have a probability distribution, taking into account the variability in crack initiation lives. In order to account for the variability in the S-N curve data (P-S-N curves), at the start of an analysis a randomly generated probability value (chance) is added to every initiation site, determining from the P-S-N data the S-N curve for that site. Thus, every simulation results in a different crack initiation pattern

The stress intensity factors of the crack growth model for the MSD situation are calculated by the use of the compounding method, in which a stress intensity factor is determined by combining the known solution of the isolated cracked hole and its boundaries (edges, other holes or cracks) separately. Through cracks are assumed, because insufficient SIF-solutions exist for corner cracks. All the SIF solutions are based on a uniform stress distribution, which is not exactly the case here. Stress redistribution, is approximated by defining a finite width determined by the remaining net-section around a crack. Load transmission due to friction is only approximately modelled.
The model is currently based on flat sheets, leaving out the influence of the curvature, e.g. different stress-state in case of bulging

All the parameters from both, the crack initiation and crack growth model, can be treated as random variables and the stochastic problem is solved currently with the Monte-Carlo method. A more advanced stochastic method based on a Second-Order Reliability Method (SORM) has been developed recently.
A common problem with stochastic analysis is to obtain reliable data concerning the random variables. The probability density curves for the random variables are hard to obtain or even unknown. Therefore, data has to be obtained from literature and serve as estimation.

The program has been applied amongst others on a sheet with 14 holes of which the outer two holes were cold worked (low probability of failure). In figure 13 the calculated crack initiation period and crack growth period are plotted against each other for 1000 MC simulations. Also, contour ellipses have been drawn representing areas within γ percentile of the data points are included, under the assumption that both the crack initiation period and crack growth period are normally distributed. The major axis of the ellipses are not horizontally orientated representing the statistically dependency between the crack initiation period and the crack growth period, i.e. the longer the initiation period the shorter the crack growth period. The experimentally obtained results are represented by triangles.
In figure 14 the crack growth patterns at the various holes are shown for the longest (MSD situation) and shortest life (no MSD situation) obtained in the numerical analysis.

1.7 FIBER METAL LAMINATES

1.7.1 Dutch GLARE Technology research program

In the Netherlands a GLARE technology research program (GTO) is carried out. GLARE is a fiber metal laminate, which was initially developed for its excellent fatigue behaviour in terms of slow crack growth properties. The material appeared to have a lot more favourable properties, such as very high impact, corrosion and fire resistance capacity.
The GTO program is co-ordinated by Structural Laminates Industries (SLI). Other participants are Technical University Delft (TU Delft), the National Aerospace Laboratories (NLR) and Fokker Aerostructures (Fe). The program is sponsored by the Dutch government and is performed in close co-operation with DaimlerChrysler Aerospace Airbus (DA).
The research aims to achieve technology readiness for the application of GLARE laminates in very large transport aircraft. To do so, projects on the following working groups have been defined:

1. Materials & Processes
2. Methods
3. Design Concepts
4. Fabrication Technology
5. Maintenance
6. Durability

More than 90 subprojects were defined and are carried out in these working groups.

1. Materials & Processes

Main topics are material qualification and material properties and allowables. Another very important issue is the definition and the qualification of the splicing concept. With these splices it is possible to manufacture larger skin panels than with monolithic aluminium sheets. An example of how a splice in a GLARE panel looks like is given in the figure 15.
It is shown that with clever design and manufacturing a considerable cost reduction can be achieved which makes GLARE a very competitive material as compared with conventional sheet materials. The laminar built-up of GLARE allows a high degree of integration of structural details in one panel, such as splices and internal doublers.

2. Methods

This subject is focussed on the development of missing calculation methods (design tools) for GLARE structures. Research is aimed at prediction of basic material properties (“metal volume fraction” approach), stability of panels, residual strength and crack propagation.

3. Design Concepts

Design principles are under development to enable detailed design optimised for GLARE structures. Items such as panel arrangement, typical GLARE shell design, stringer design concepts, longitudinal and butt joints, door and window cut-outs are looked upon. Also certification aspects are under discussion.

4. Fabrication Technology

This subject is focussed on low cost and low risk manufacturing of GLARE fuselage skin panels. Although the actual material cost of GLARE is higher than for monolithic aluminium,

5. Maintenance

Maintenance concepts (with emphasis on cost aspects) and NDT inspection and repair methods for GLARE structures are under development. A lot of effort has been put into successful activities to acquire airline acceptance of GLARE.

6. Durability

Available test results show excellent properties related to durability of GLARE, but a large durability program is defined to take away some reservations, which still exist at aircraft manufacturers and operators.

A very interesting feature is the relation between reduction in mechanical properties due to environmental influences and the amount of downscaling to coupons and components. The more a test article resembles with the actual structure, the less the reduction of mechanical properties there will be.

1.7.2 Repair with bonded fibre metal laminate patches (A. Woerden, A. Vlot, TU Delft)

Because of ageing aircraft a need exists for safe, damage tolerant and cost-effective repairs. Different repair techniques are available, including mechanically fastened patch repairs and adhesive bonded patch repairs. Bonded repairs provide a more uniform and efficient load transfer into the patch and avoid high stress concentrations caused by additional holes necessary for riveted repairs. Adhesive bonded boron/epoxy repairs have the disadvantage of a large mismatch in coefficient of thermal expansion (CTE) between the repair and the aircraft structure. Moreover, the very high stiffness of boron/epoxy can lead to load attraction problems on the repair. Fiber Metal Laminate (FML) repair materials like GLARE® (GLAss REinforced) avoid these problems. Research into bonded repair FML repairs patches started in the early nineties between the Center for Aircraft Structural Life Extension (CAStLE) at the United States Air Force Academy (USAFA) and the Structures and Materials Laboratory of the Faculty of Aerospace Engineering of Delft University of Technology in the Netherlands. Considerable research performed over the last years resulted in a better understanding of the physical background of bonded repairs, as well as significant improvements in bonded repair techniques. Current research focuses on the ability to accurately predict the crack driving stress intensity factor (ΔK) at the crack tip of a crack under an adhesively bonded repair. This ΔK is significantly lower than for an unrepaired crack, explaining the excellent fatigue behaviour of bonded repairs, as shown in the figure 16 with crack growth curves. This research is performed for both boron/epoxy and GLARE® patch repair materials. Models being used for the prediction of ΔK include analytical models like the Rose model and finite element models. The Rose model gives an excellent analytical background, but secondaries bending for one-sided (i.e. asymmetrical) repairs and thermal stresses after curing are not accurately accounted for. Extensive experimental testing, see figure 17 with barrel test set up, and finite element calculations are performed to investigate the influence of those two main variables, and to extend previous modelling.
Another part of current research focuses on in-service effects on patch performance and the experimental testing of realistic load sequences (variable-amplitude loading), including effects of overloads and underloads on crack growth of the repaired crack.
Research on in-service effects on patch performance, as yet hardly investigated, will concentrate on environmental influences on crack growth under a patch repair and on the growth of debonds between patch and adherent. Possible detrimental environments include cold, hot, humid and salty conditions, as well as combinations of those. In view of service experience, two bonded GLARE patches were installed on a C5-A Galaxy, which are inspected regularly.
A final goal of the “Repair Project” is the development of a repair tool for maintenance engineers, requiring little background knowledge of bonded repair. A first version of this tool, called CalcuRep® needs to be updated to accurately account for effects of secondary bending, influence of thermal stresses due to the curing cycle and effects of different environmental conditions.

1.7.3 Spliced Fibre Metal Laminates (T.J. de Vries and A. Vlot, TU Delft)

The maximum sheet width for 0.3 mm thick aluminium, and thus for GLARE laminates with this type of aluminium layers, is approximately 1.65 m. However, for the purpose of skin material in a fuselage, wider sheets are preferred to reduce the amount of necessary joints. This problem can be solved with the splicing concept; metal sheets are interrupted in the laminate and these splices are bridged by the fiber layers, see figure 18. With this concept the sheet width can be increased to 4 meters or more, depending on the autoclave size. Using these large sheet sizes can provide an additional weight and cost saving compared to monolithic aluminium structures due to a reduction of the number of riveted joints.
Fatigue and static strength tests on spliced laminates with varying fibre orientation were performed to determine design allowables. The disadvantages of local cross section reduction and the possible influence of moisture, which can penetrate in the uncovered splice, can be solved by covering the splice with a doubler. Bonding the doubler with prepreg over the splice appeared to be not favourable because of the low delamination resistance of the prepreg layer.

Possible solutions to maintain a smooth aerodynamic surface, even with bonded doublers, are now under development. Residual strength tests on spliced laminates with through cracks showed that the splices can effectively stop stable crack extension. In this case the crack has to reinitiate at the other side of the splice.

1.7.4 Service trial of a GLARE crownpanel in the A310 fuselage (N.J. Fraterman, Fokker Aerostructures)

An existing Airbus A310 will be installed with a large cargo door in the forward fuselage for a German customer. During the installation of this large door an Aluminium fuselage panel in the pressurised crown just aft of the door will be replaced by a GLARE panel. The installation of this GLARE panel is a service trial in order to gain more experience with GLARE in wide body aircraft under real loading and environmental conditions. The GLARE panel has the dimensions of 1600 x 4000 mm, is equipped with bonded Aluminium stringers and is attached to the existing frames with clips.

For the certification programme a number of static and fatigue tests on representative coupons of the panel will be performed. The fatigue tests include the circumferential and longitudinal lap joint of the GLARE panel to the existing surrounding structure and will be performed with a representative load spectrum. For some specimens also the environmental conditions (hot, wet) will be taken into account.

1.8 NON-DESTRUCTIVE INSPECTION

1.8.1 Inspection procedures (A. Oldersma, J.H. Heida, NLR)

For a number of RNLAF in-service inspection points of the F-16 airframe the detection of fatigue cracking led to a non-destructive and destructive evaluation of the parts concerned. The cause and extent of fatigue cracking was determined and, subsequently, changes in the inspection procedures of for example the Nose Landing Gear NLG shock strut piston radius and the flaperon root rib radius were proposed.

1.8.2 Reliability of inspection (J.H. Heida, F.P. Grooteman, NLR)

The possibilities within the Royal Netherlands Air Force (RNLAF) maintenance system to establish reliability data relevant for the in-service nondestructive inspection of F-16 airframe structure have been investigated. The principal inspection techniques herewith are manual and automatic eddy current inspection for the detection of fatigue cracking. Use was made of field inspection data registered in the Core Automated Maintenance System (CAMS) for specific airframe inspection points within the F-16 Aircraft Structural Integrity Program (ASIP). The available data include the registration of the number of cracks and the length of the largest crack found during the phased inspections. Further, use was made of crack growth data obtained from the aircraft manufacturer. An evaluation of the field inspection data and the crack growth data allows the estimation of the sensitivity and reliability of inspection for the structural details concerned, by constructing the Cumulative Distribution Function (CDF) of the detected crack sizes. An example of this approach is given in figure 19. The results of this evaluation can be used to revise the current values of the inspection intervals for the ASIP inspection points.

1.9 References

1. Spiekhout D.J., F-16 loads/ usage monitoring. RTO meeting ‘Exploitation of structural loads/ health data for reduced life cycle costs’ Brussels May 1998, RTO-MP-7.
2. Arts T., Lambert de Rouvroit M., Rutherford A.W., Aero-thermal investigation of a highly loaded transonic linear turbine guide vane cascade, Technical note 175, Von Karman Institute for Fluid Dynamics, 1990.
3. Koolloos, M.F.J. and J.M. Houben, Behavior of Plasma Sprayed TBCs During Thermal Cycling and the Effect of a Pre-Oxidised NiCrAlY Bond Coat, to be published in *Journal of Thermal Spray Technology*, 1999.

4. Fawaz, S.A., Fatigue crack growth in riveted joints. Doctor thesis, Delft University of Technology, 2 Sept 1997.
5. Fawaz, S.A. and Schijve, J., Fatigue crack growth predictions in riveted joints. Proceedings 2nd joint NASA/FAA/DoD Conference on Ageing Aircraft, Williamsburg, 31 Aug-3 Sept. 1998.
6. Schijve, J., The significance of fractography for investigations of fatigue crack growth under variable-amplitude loading. Delft University Press, Series 07: Aerospace Materials 09, 1998.

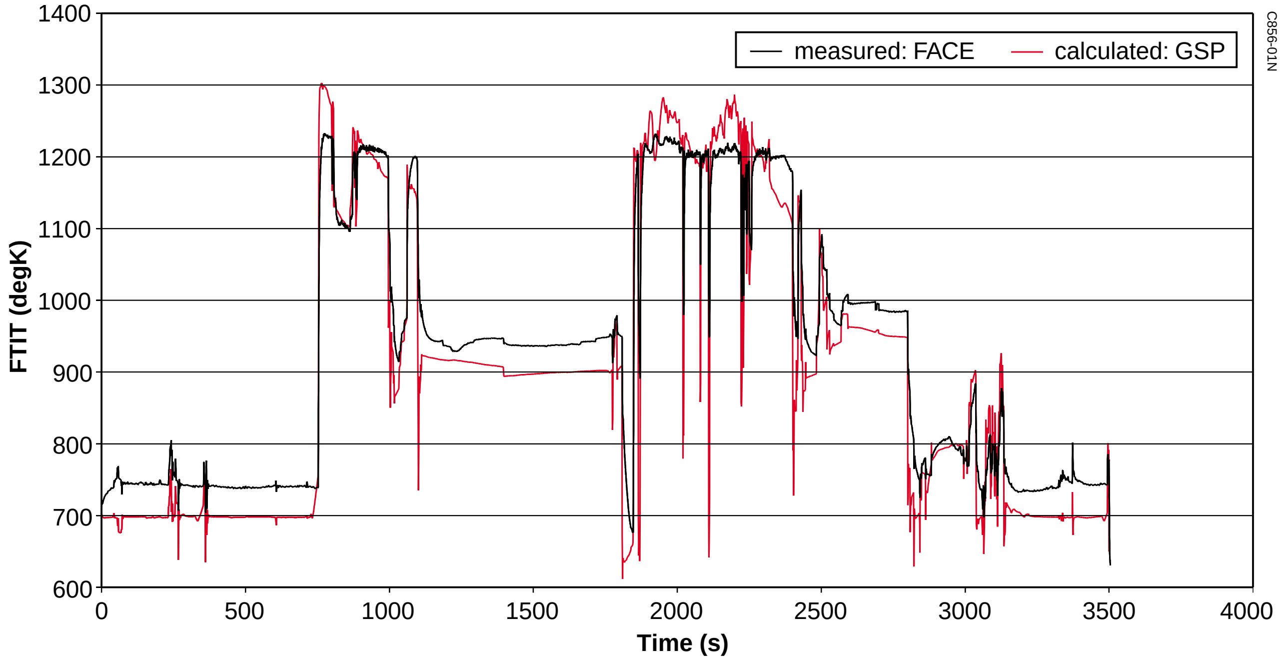

Figure 1 **Comparison of fan turbine inlet temperature (FTIT) values during a mission as measured by FACE and calculated by GSP**

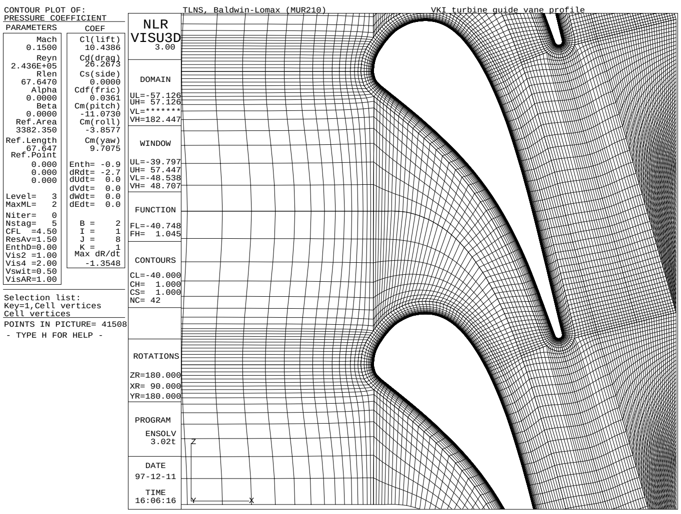

Figure 2 **2D turbine blade cascade. Von Karmen Institute experiments are used for CFD validation**

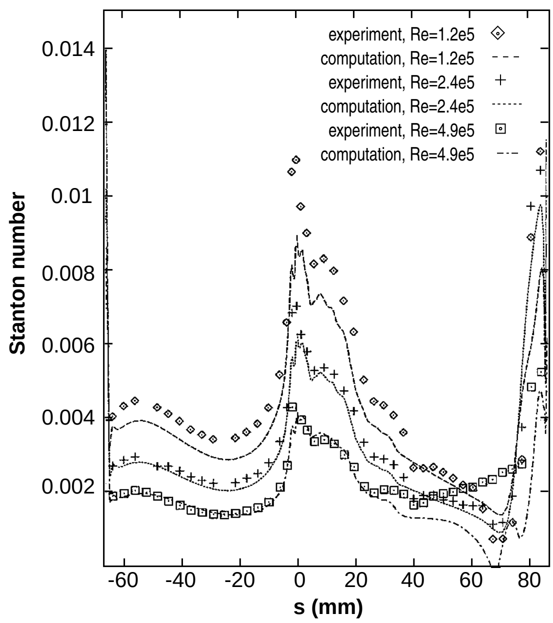

Figure 3 **Calculated and measured heat transfer (represented by the Stanton number)**

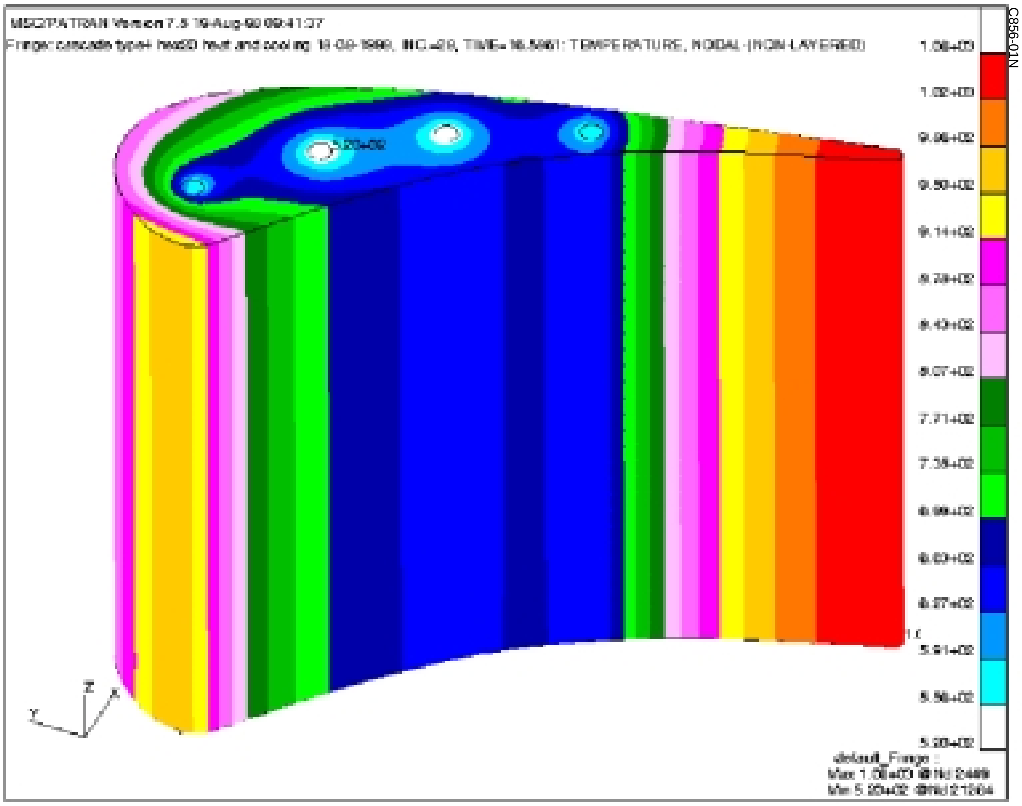

Figure 4   Steady state temperature distribution calculated for an internally cooled blade

Figure 5   Thermal stresses calculated for an internally cooled blade

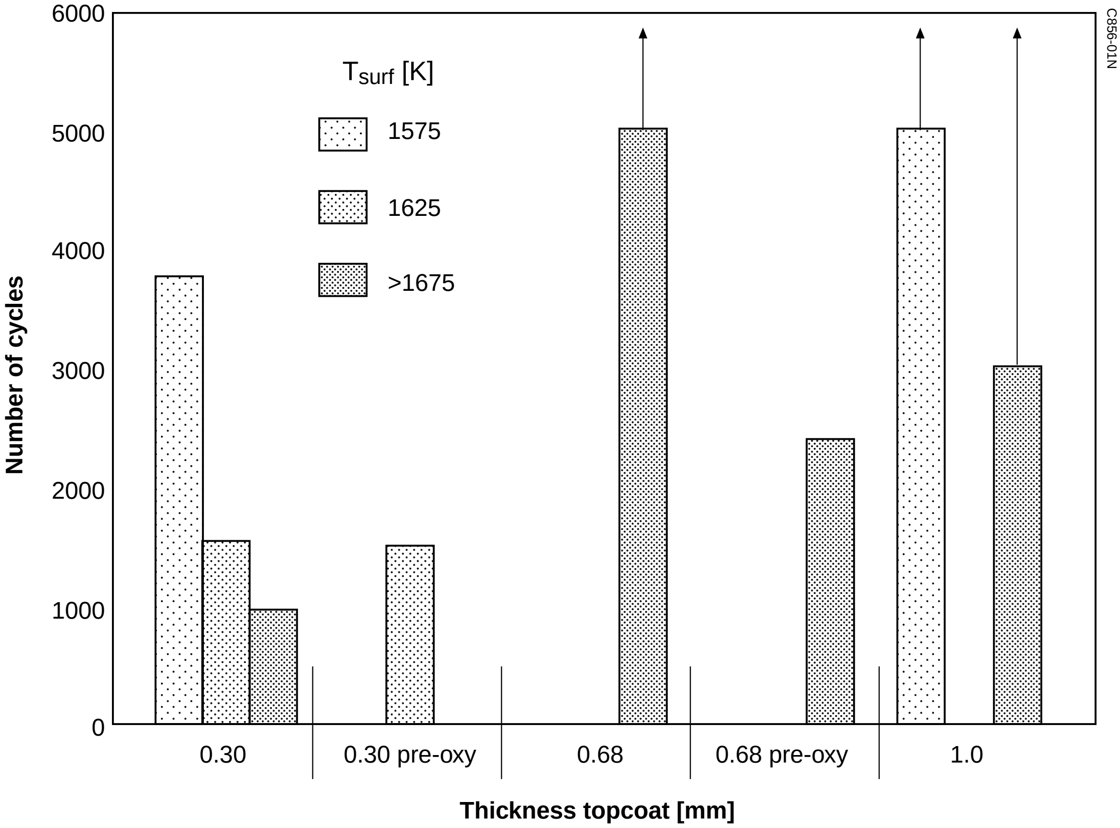

Figure 6 Number of thermal shock cycles to failure for several test temperatures, and for 0.3 and 0.68 mm (with and without pre-oxidized bond coat) and 1.0 mm specimens. Arrow an top of bar indicates that delamination did not ocur withn given number of cycles

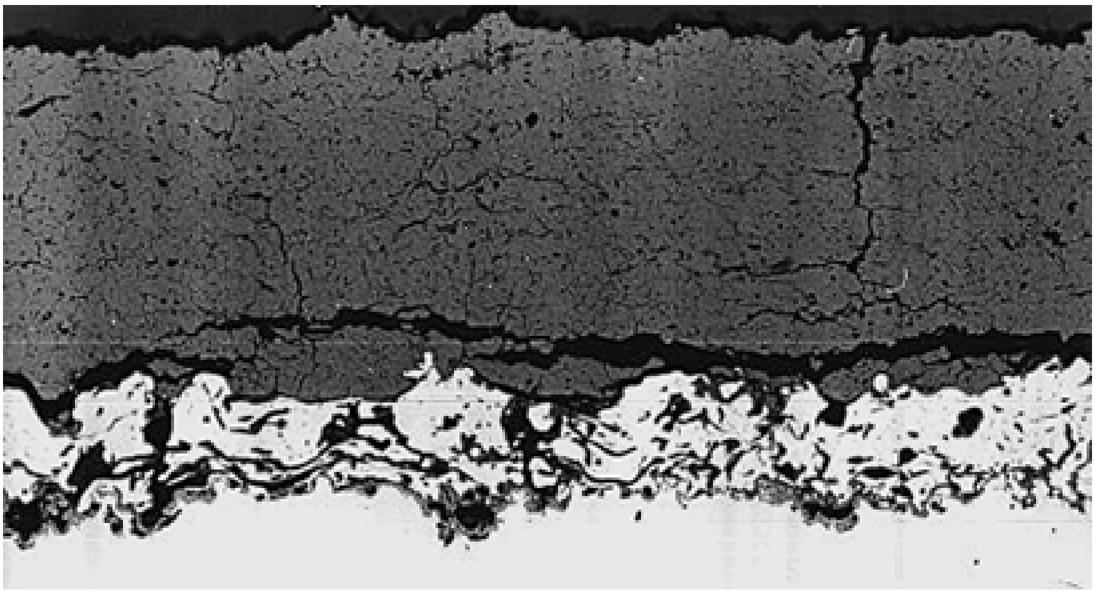

Figure 7 Failure mode of a TBC coating after thermal shock cycles

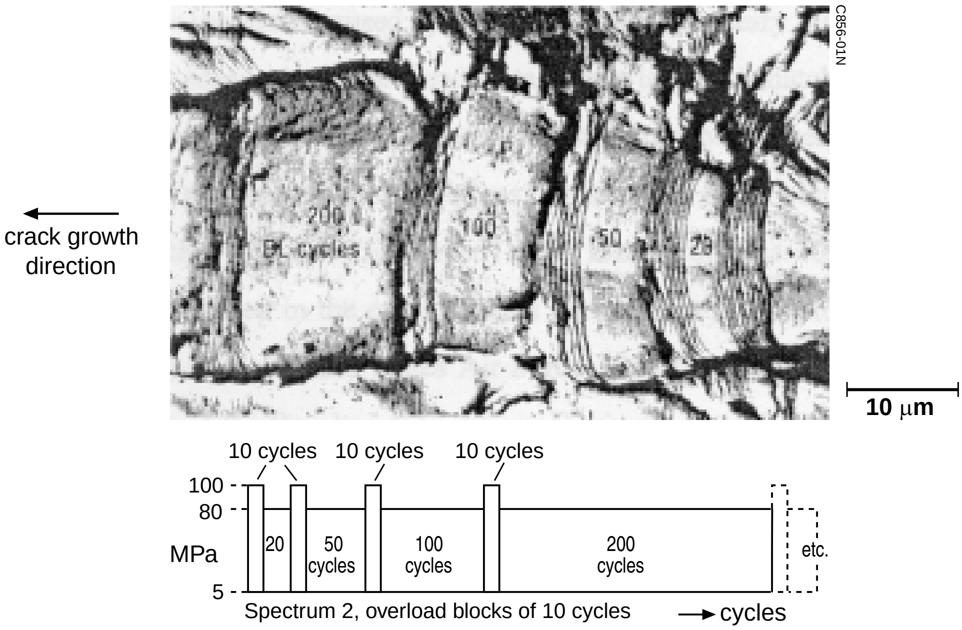

Figure 8 Overload cycle striations can easily be observed. The width of the intermediate bands of the baseline cycles is not proportional to the numbers of baseline cycles, which indicates a retardation effect

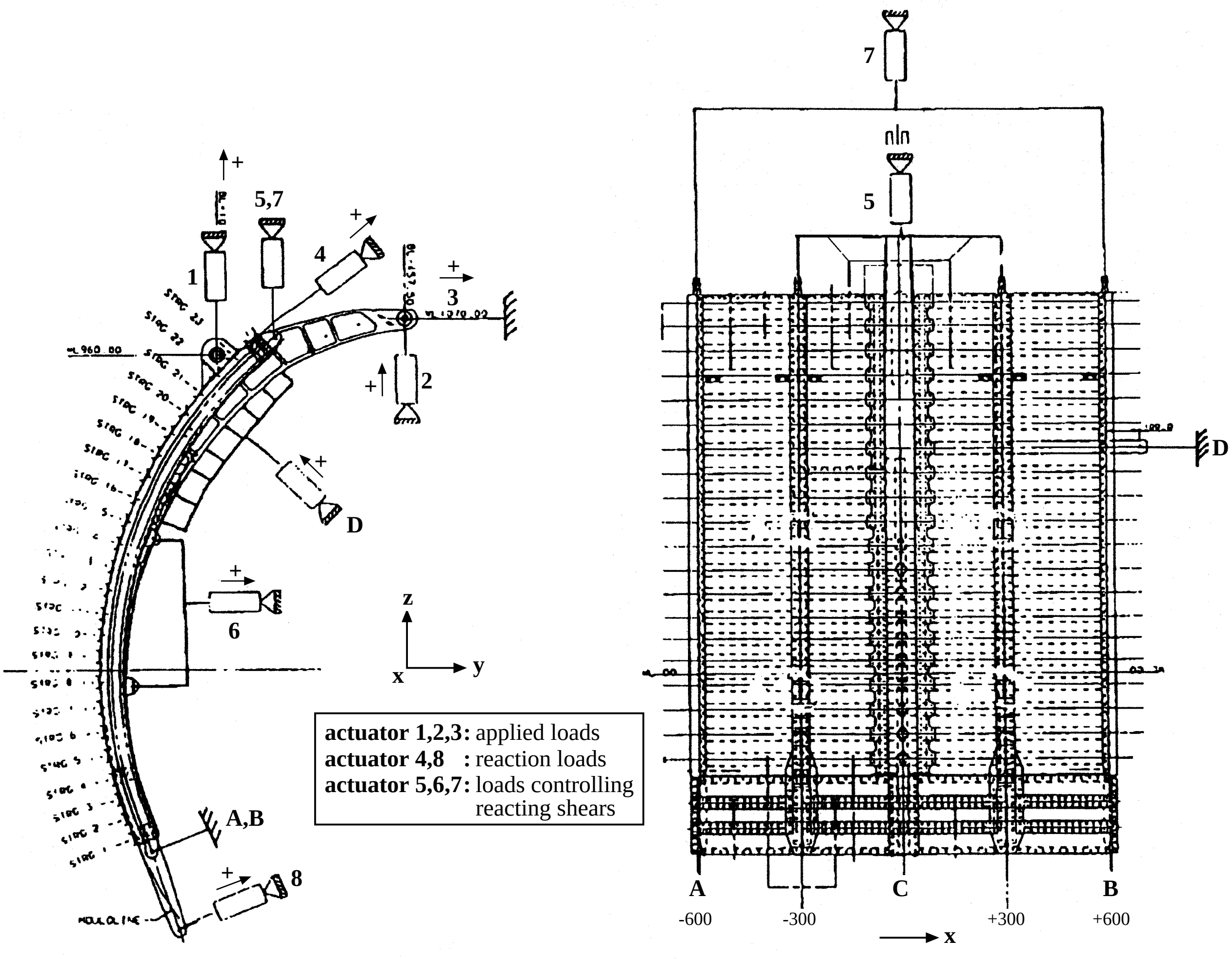

Figure 9 Fokker 60 wingfuselage connection; mainframe componenttest

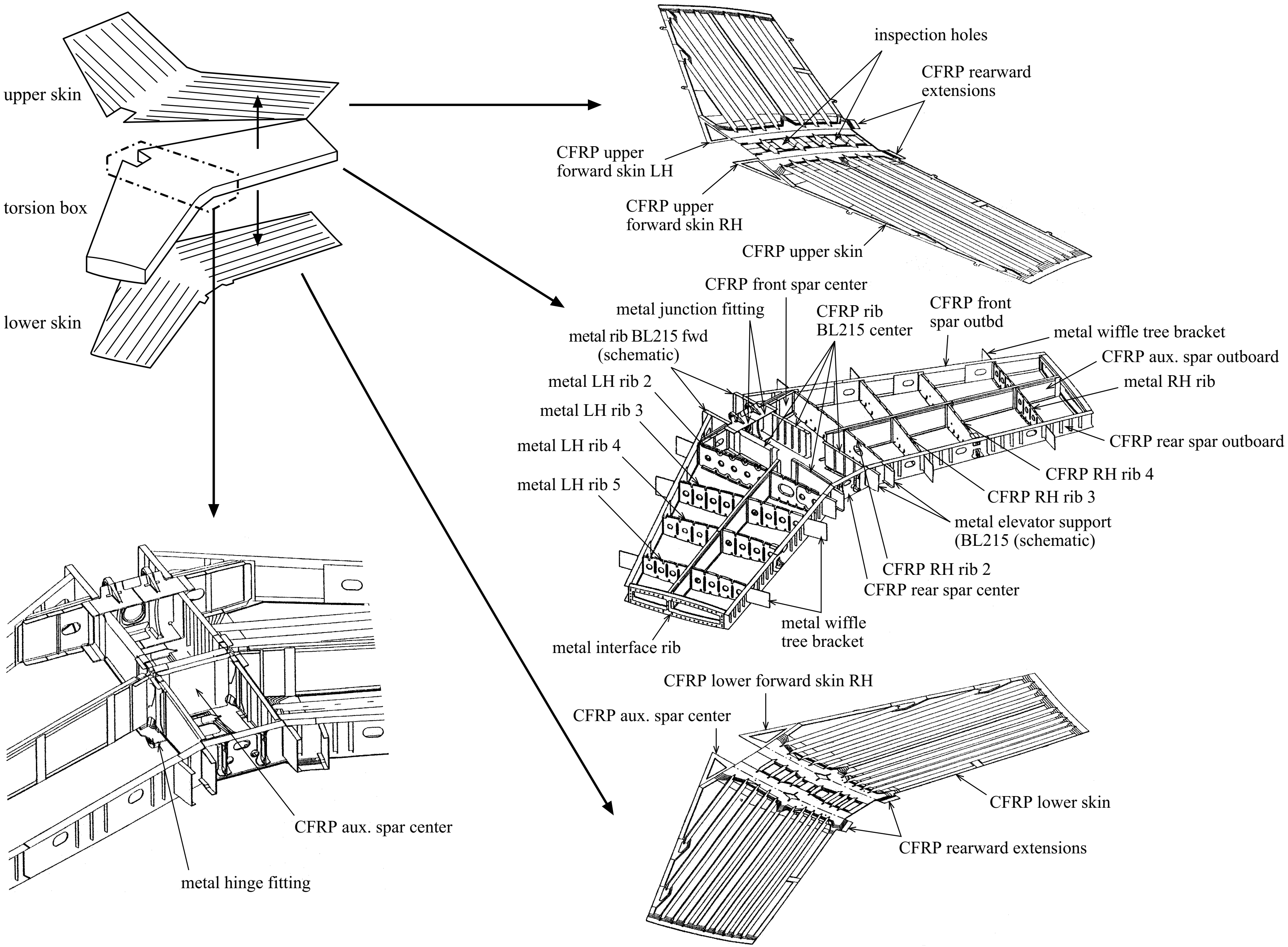

C856-01N

Figure 10 Structural lay-out of the "4-meterbox"

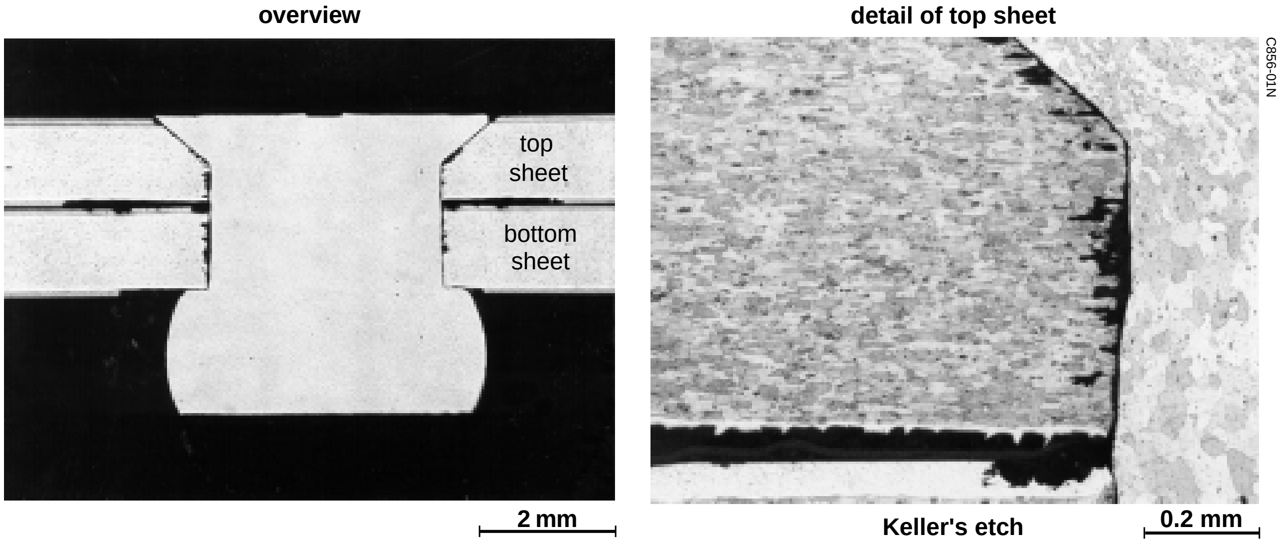

Figure 11 Cross section of a riveted top and bottom sheet

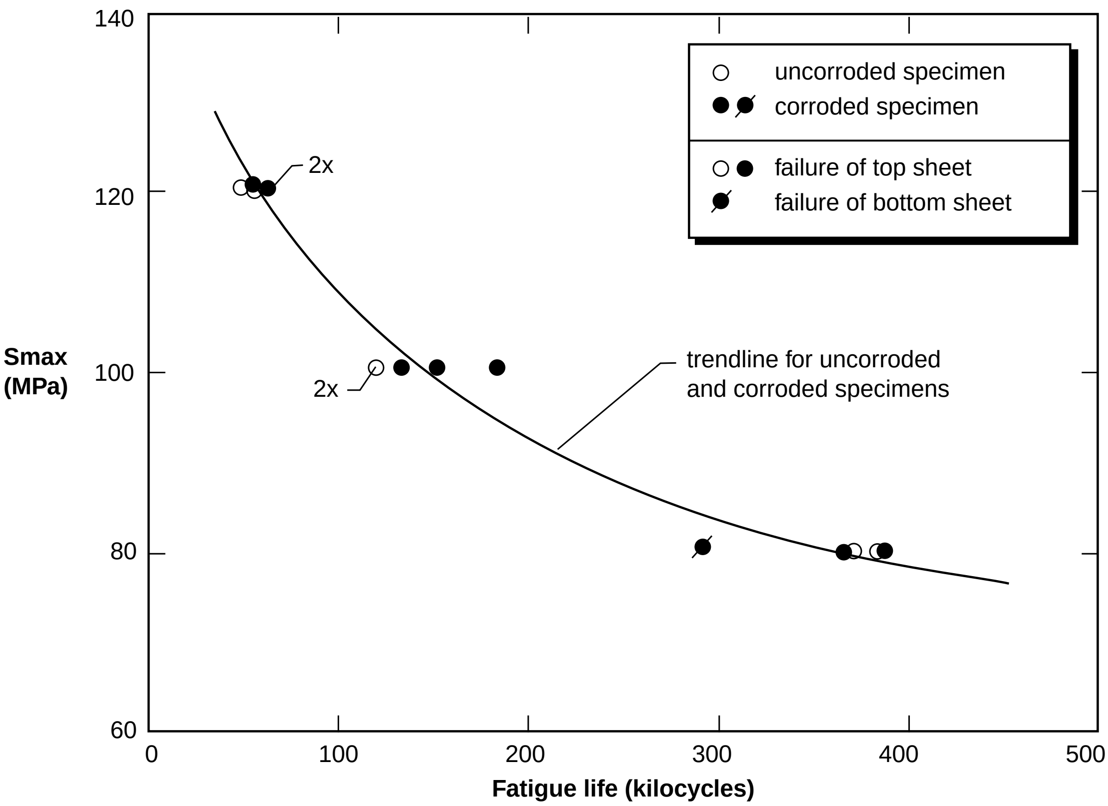

Figure 12 Fatigue lives as a function of maximum stress for uncorroded and corroded lap joint specimens, R=0.1

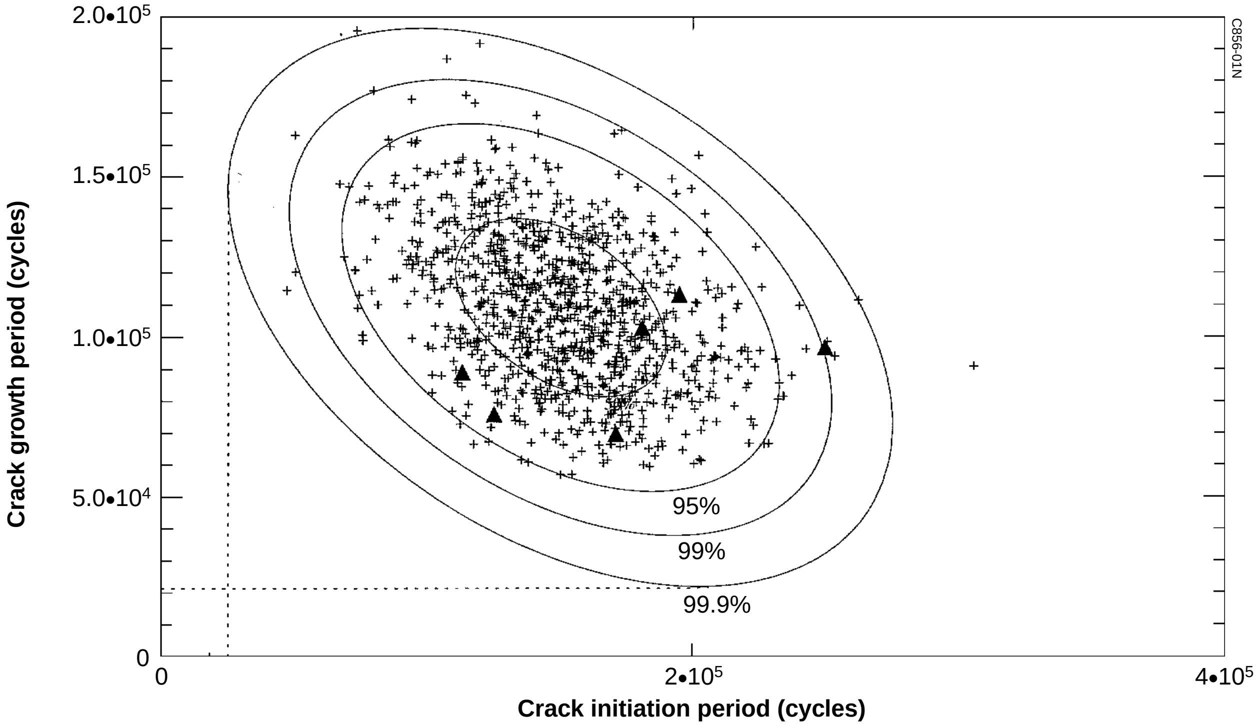

Figure 13 Crack initiation period versus crack growth period: numerical and experimental results

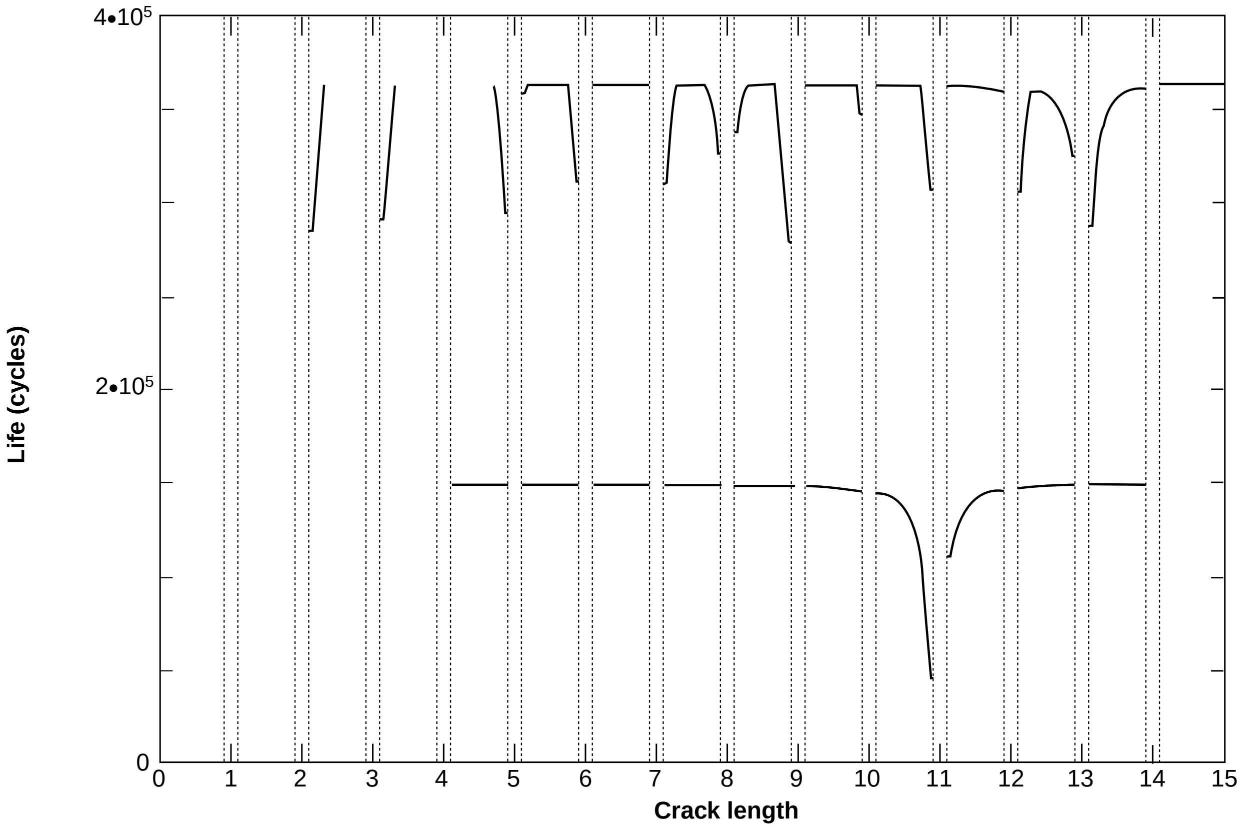

Figure 14 Crack growth pattern at the varous rivets for the shortest and longest life obtained

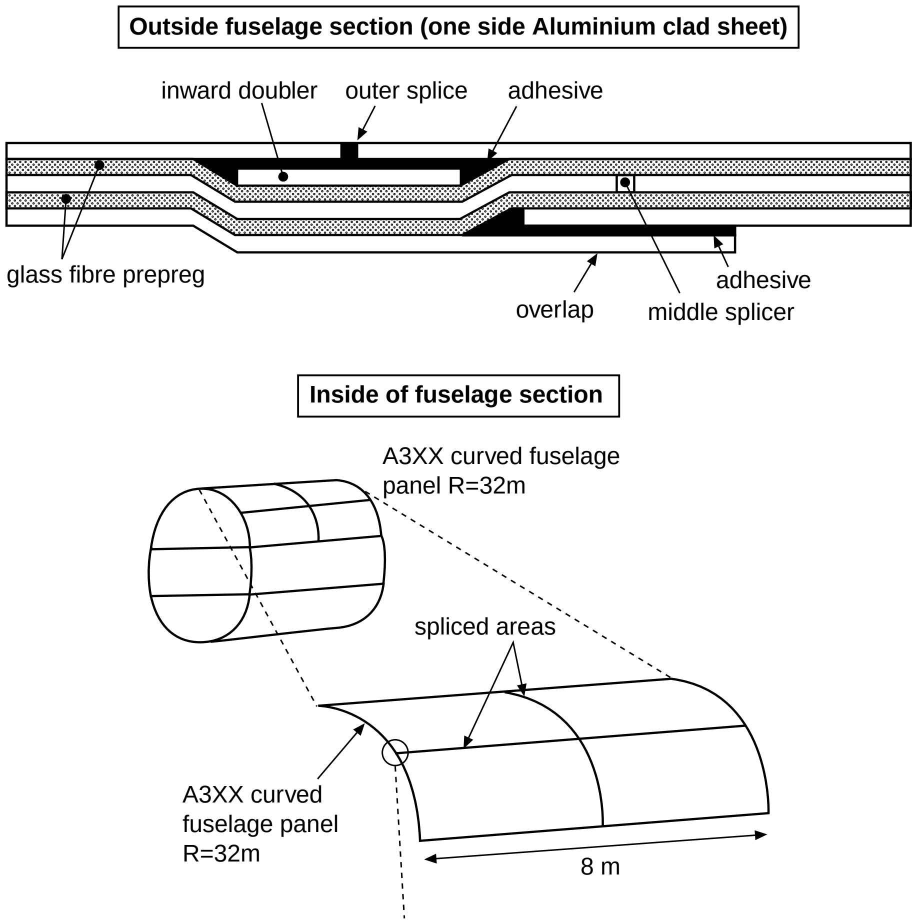

Figure 15 Splices in GLARE fuselage panels

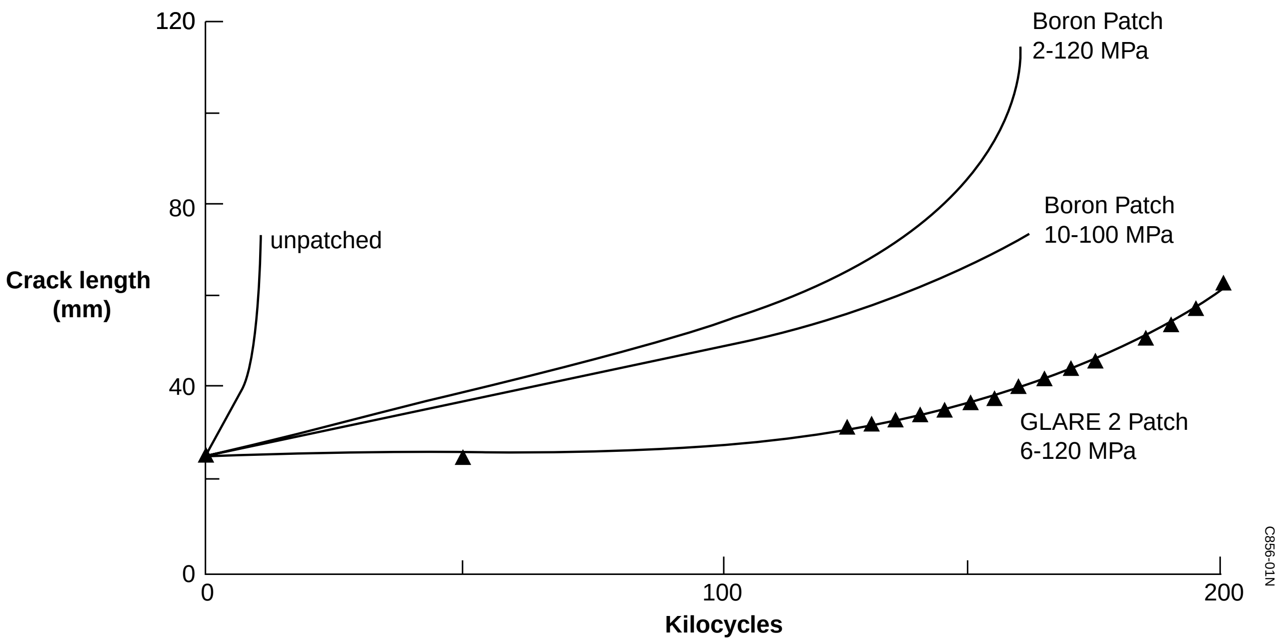

Figure 16 Crack growth curve for unrepaired and different adhesively bonded repairs

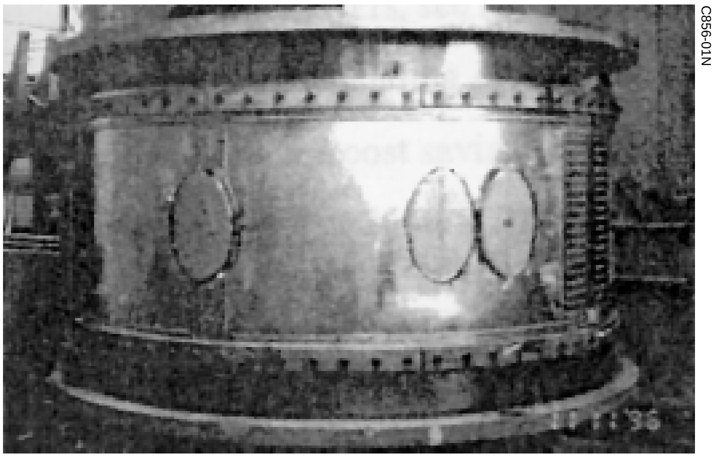

Figure 17 Example of experimental testing: barrel test setup

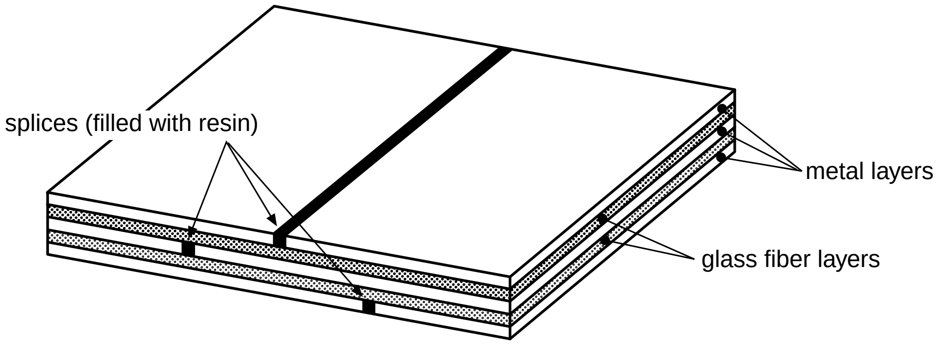

Figure 18 A spliced joint

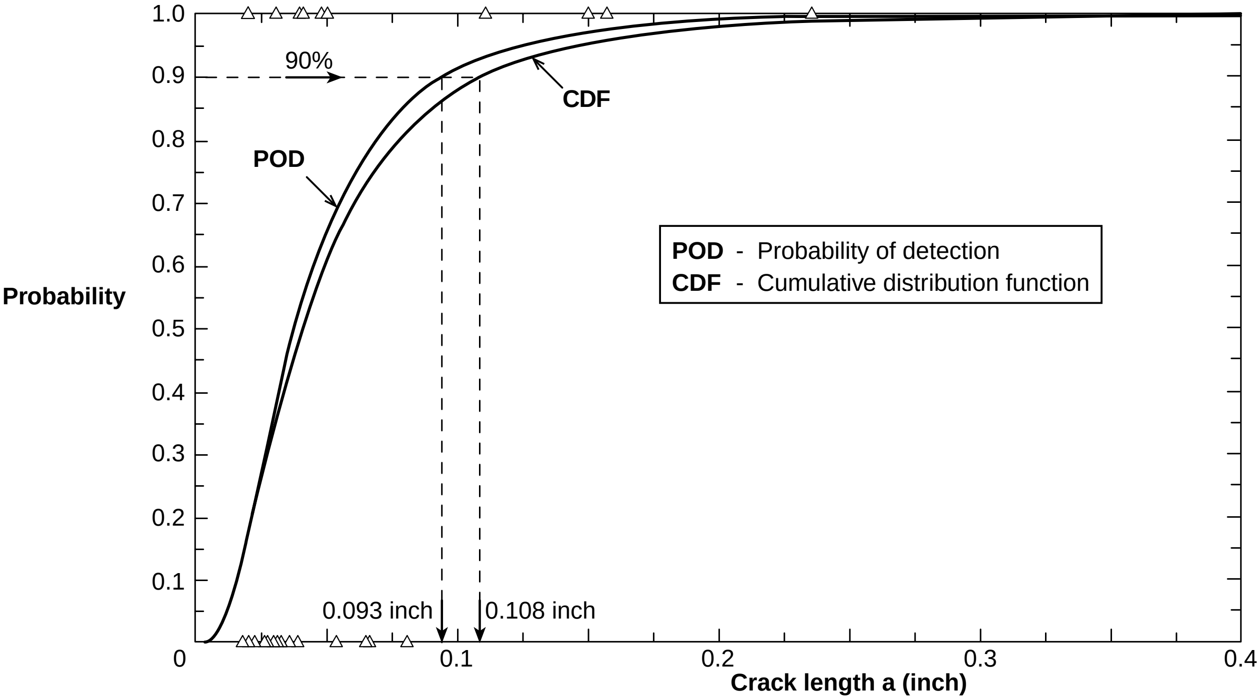

Figure 19 CDF of 28 "hit"data points and mean POD curve of 64 "hit/miss" data points for the manual eddy current inspection of a specific F-16 ASIP point